

See discussions, stats, and author profiles for this publication at: <https://www.researchgate.net/publication/231231536>

Design and Growth of Quaternary Mg and Ga Codoped ZnO Thin Films with Transparent Conductive Characteristics

ARTICLE *in* CRYSTAL GROWTH & DESIGN · SEPTEMBER 2011

Impact Factor: 4.89 · DOI: 10.1021/cg2005387

CITATIONS

25

READS

43

8 AUTHORS, INCLUDING:



Seung Wook Shin

University of Minnesota Twin Cities

90 PUBLICATIONS 1,064 CITATIONS

SEE PROFILE



In Y Kim

Hanyang University

265 PUBLICATIONS 4,272 CITATIONS

SEE PROFILE



Ganesh Agawane

Korea Photonics Technology Institute

55 PUBLICATIONS 611 CITATIONS

SEE PROFILE



Jin Hyeok Kim

Chonnam National University

164 PUBLICATIONS 1,487 CITATIONS

SEE PROFILE

Design and Growth of Quaternary Mg and Ga Codoped ZnO Thin Films with Transparent Conductive Characteristics

Seung Wook Shin,[†] In Young Kim,[‡] Gyoung Hoon Lee,[‡] G.L. Agawane,[‡] A.V. Mohokar,[§] Gi-Seok Heo,^{||} Jin Hyeok Kim,^{*,‡} and Jeong Yong Lee^{*,†}

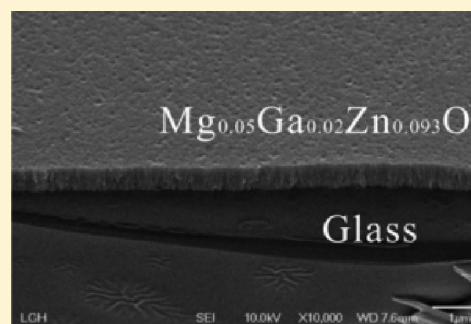
[†]Department of Materials Science and Engineering, KAIST, 335 Gwahangno, Yuseong-gu, Daejeon, 305-701, South Korea

[‡]Photonics Technology Research Institute, Department of Materials Science and Engineering, Chonnam National University, 300 Yongbong-Dong, Buk-Gu, Gwangju 500-757, South Korea

[§]Department of Physics, Shivaji University, Kolhapur 416 004, M.S., India

^{||}Development of Advanced Components & Materials, Korea Institute of Industrial Technology, Gwangju, 500-480, South Korea

ABSTRACT: This study reports the design growth and characterization of quaternary Mg and Ga codoped ZnO (MGZO) thin films with transparent conductive characteristics deposited on glass substrates by RF magnetron sputtering. The effects of the Ga concentration (from 0 to 2 at %) on the structural, chemical, morphological, optical, and electrical properties of MGZO thin films were investigated. X-ray diffraction study showed that all the MGZO thin films were grown as a polycrystalline hexagonal wurtzite phase with a *c*-axis preferred orientation and random in-plane orientation. The 2θ value of the (0002) peak of MGZO thin films decreased with increasing Ga concentration. X-ray photoelectron spectroscopy confirmed the Mg and Ga binding energy peaks from the MGZO thin films. The MGZO thin films had a smoother surface morphology. The optical study showed that the band gap energy of MGZO thin films systematically increased from 3.25 to 3.75 eV with increase Ga concentration. The electrical resistivity of the MGZO thin films was improved from 9.5×10^{-2} to $6.89 \times 10^{-4} \Omega \text{ cm}$ with increasing Ga concentration.



1. INTRODUCTION

Zinc oxide (ZnO) is a promising candidate as transparent conducting oxide (TCO) owing to its low cost, relatively low deposition temperature and stability in hydrogen plasma compared to ITO and SnO₂,^{1,2} which have been the most popular TCO materials. Unfortunately, undoped ZnO thin films have a relatively high resistivity ($10^{-2} \Omega \text{ cm}$) and optical band gap energy (3.3 eV), which limits its use for electro-optical applications due to the low carrier concentration.³ To utilize ZnO-based materials in optical and electrical devices with high performance and reliability, it is necessary to control the optical band gap engineering and electrical properties of ZnO thin films.⁴ Magnesium oxide (MgO) is a promising material for optical band gap engineering of ZnO. Mg-doped ZnO (MZO) thin films formed by alloying ZnO with MgO showed that the band gap energy varies with the Mg concentration.⁵ Many studies have examined the band gap engineering of MZO thin films using various techniques.^{5,6} These researches on the MZO thin films indicated that the crystal structure of MZO thin films can be changed from a hexagonal structure to cubic structure when the Mg concentration exceeds 40 at % and the optical band gap energy of MZO varies from 3.3 to 4.0 eV without a phase change. The wider band gap energy of MZO thin films have the several advantages in the n-type layer for light emitting diodes (LEDs), buffer and TCO layers for thin film solar cells (TFSCs).^{7,8} R. Schmidt-Grund et al.⁹ have forecasted the improved exciton binding energy in the MZO materials with increasing Mg

concentration, which lead to the development of new n-type MZO/p-type GaN-based heterojunction LEDs that would be useful in the ultraviolet region. On the other hands, the MZO thin film with a wider band gap energy results in improved conversion efficiency in chalcopyrite-based TFSCs because the conduction band offset (CBO) of Cu(In,Ga)Se₂ (CIGS) multistructured device is minimal and the absorption of buffer layer is reduced in the short wavelength region.⁸ Recently, Mimemoto et al.¹⁰ and S. Shimakawa et al.⁸ reported that MZO thin films can be used as a buffer layer in CIGS-based TFSCs. These reports suggest that the CBO values of the MZO buffer and CIGS absorber layer can be controlled by changing the band gap energy, resulting in improved conversion efficiency as compared to that of CdS. Although the CBO and conversion efficiency of CIGS-based TFSCs are improved by the introduction of MZO as a buffer layer between the absorber and window layers, the band gap energy misalignment problem of n-ZnO (3.5 eV)/MZO (3.6–3.8 eV)/CIGS (1.2 eV)/Mo/Glass structure in the CIGS-based TFSCs remains to be unsolved. To solve this problem, it is important to control the band gap energy of the individual layers of TFSCs or to introduce new window materials with a band gap energy (over 3.8 eV) wider than that of the buffer layer and a low resistivity below $10^{-3} \Omega \text{ cm}$.

Received: April 28, 2011

Revised: August 17, 2011

Published: September 06, 2011

On the other hand, the optical and electrical properties of ZnO thin films can be improved by Ga-doping ZnO structure^{11,12} because of its superior merits, such as more resistant to oxidation and similar ionic radius to Zn^{2+} ions than other impurities, which minimizes the ZnO lattice deformations, even at higher concentrations.^{2,3} Our previous papers on Ga-doped ZnO (GZO) thin films showed that the polycrystalline GZO thin films with outstanding electrical resistivity varying from $4.9 \times 10^{-3} \Omega \text{ cm}$ to $1.4 \times 10^{-4} \Omega \text{ cm}$ ^{13,14} can be developed. Nevertheless, the band gap energy of GZO thin films is limited above 3.6 eV without changing the crystal structure. Some researchers have examined Ga and Mg codoped ZnO (MGZO) thin films to solve the problem of band gap misalignment in TFSCs, and improve the electrical resistivity and optical band gap energy of the window layer.

However, there are no reports on systematic controlling of the optical band gap energy and electrical resistivity for MGZO thin films with different Ga concentrations. This paper reports MGZO thin films deposited on glass substrates by RF magnetron sputtering. The effect of the different Ga concentration (0–2 at %) on the structural, chemical, morphological, optical, and electrical properties of MGZO thin films was studied.

2. EXPERIMENTAL DETAILS

Pure ZnO, MZO, and MGZO thin films were prepared on glass substrates by RF magnetron sputtering with different Ga concentrations from 0 to 2 at %. The Mg concentration in the MGZO thin films was fixed to 5 at %. The ceramic ZnO, MZO, and MGZO targets were prepared using a conventional solid-state reaction method. The mixture, which was made from high purity ZnO powder (99.99%) and the desired amount of high purity Ga_2O_3 (99.99%) and MgO powders (99.99%), was pressed using a cold isostatic press (CIP) and sintered at 1100 °C for 4 h. Prior to the deposition of pure ZnO, MZO, and MGZO thin films, the glass substrates were cleaned ultrasonically with acetone, methanol, isopropyl alcohol, and deionized water for 10 min. The cleaned substrates were dried by blowing with N_2 (99.99%) gas before being introduced into the sputtering chamber. The chamber was evacuated to a base pressure of 4.9×10^{-6} Torr, and the substrates were then heated to growth temperature of 350 °C. High-purity Ar gas (99.99%) was used as the plasma source, and the gas flow rate was controlled at 40 sccm using a MFC (mass flow controller). A RF power of 175 W and working pressure of 6 mTorr were used for deposition. The thickness of the deposited films (600 nm) was controlled using different deposition times for the individual films.

The crystal structure of the deposited thin films was examined by high-resolution X-ray diffraction (XRD, X'pert PRO, Philips, Eindhoven, Netherlands) operated at 40 kV and 30 mA using Ni-filtered Cu K α radiation [$\lambda = 1.54056 \text{ \AA}$]. The chemical binding energy and atomic ratios of the deposited thin films were confirmed by X-ray photoelectron spectroscopy (XPS, VG Multilab 2000, ThermoVG Scientific, UK) and electron probe microanalysis (EPMA, EPMA-1600, Shimadzu, Japan) at room temperature. The morphology of the deposited thin films was observed by field emission scanning electron microscopy (FE-SEM, Model JSM-6701F, JEOL, Japan). The optical transmittance of the deposited thin films was observed by UV–visible spectroscopy (Cary 100, Varian, Mulgrave, Australia). The electrical properties of the deposited thin films were characterized by Hall Effect measurements in Van der Paw configuration (M/N #7707_LVWR, Lake Shore Cryotronics Inc., U.S.A.) operated at room temperature.

3. RESULTS AND DISCUSSION

Figure 1 shows the XRD patterns (a) and (0002) peak positions (b) of the pure ZnO, MZO, and MGZO thin films deposited with

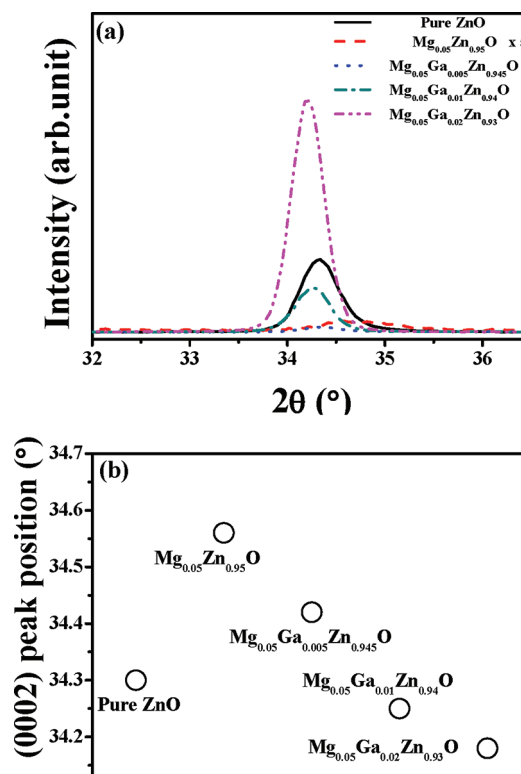


Figure 1. XRD patterns (a) and (0002) peak position (b) of the pure ZnO, MZO, and MGZO thin films deposited at different Ga concentration.

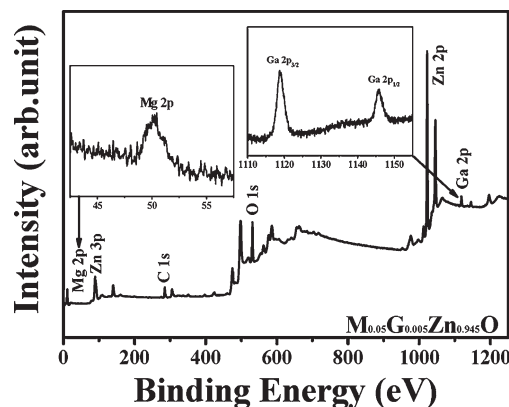


Figure 2. High-resolution XPS spectra of the $\text{M}_x\text{Ga}_y\text{Zn}_z\text{O}$ ($x = 0.05$, $y = 0.005$, and $z = 0.945$) thin films with two inset figures showing Mg 2p and Ga 2p core levels.

different Ga concentration. The (000 l) peaks of pure ZnO, MZO, and MGZO thin films (Figure 1a) were observed at $\sim 34.5^\circ$, indicating that the films were a polycrystalline hexagonal wurtzite ZnO phase with a highly c -axis out-of-plane orientation and random in-plan orientation. No metallic Mg, Ga, and Zn characteristic peaks were observed. The peak intensity of the (0002) plane for MGZO thin films were higher with increasing Ga concentration and were higher than that of pure ZnO and MZO thin films. These implied that the impurities including Mg and Ga were stabilized the MGZO structure. No other peaks from any other secondary phases, such as MgO, MgGa_2O_4 , Ga_2O_3 , and

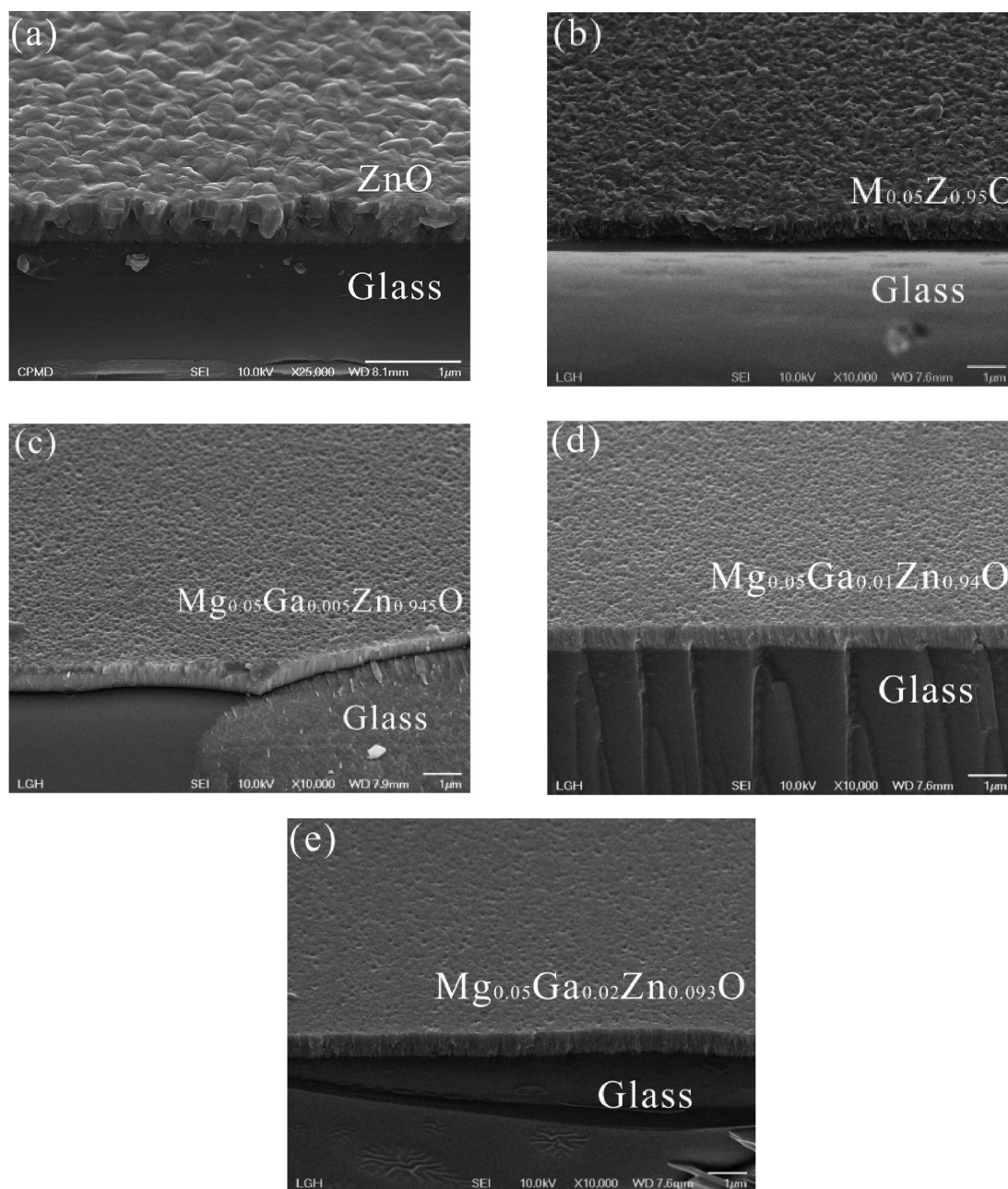


Figure 3. Cross-sectional tilted view FE-SEM images of the pure ZnO, MZO, and MGZO thin films deposited at different Ga concentrations.

ZnGa_2O_4 , were observed. The peak positions of the (0002) plane (Figure 1b) of MZO and MGZO thin films slightly shifted toward a lower diffraction angle with increasing Ga concentration. This was attributed to the different ionic radii of Ga^{3+} (0.062 nm), Mg^{2+} (0.057 nm), and Zn^{2+} (0.060 nm), respectively.^{4,15} From these different ionic radii of Ga^{3+} , Mg^{2+} , and Zn^{2+} , it was suggested that Ga^{3+} and Mg^{2+} ions substitute for Zn^{2+} ions in the hexagonal ZnO crystal structure. Previous reports on MZO and GZO thin films showed that the peak position of the (0002) plane for films shifted toward a lower or higher angle with increasing Mg or Ga concentrations, respectively.^{4,15,16}

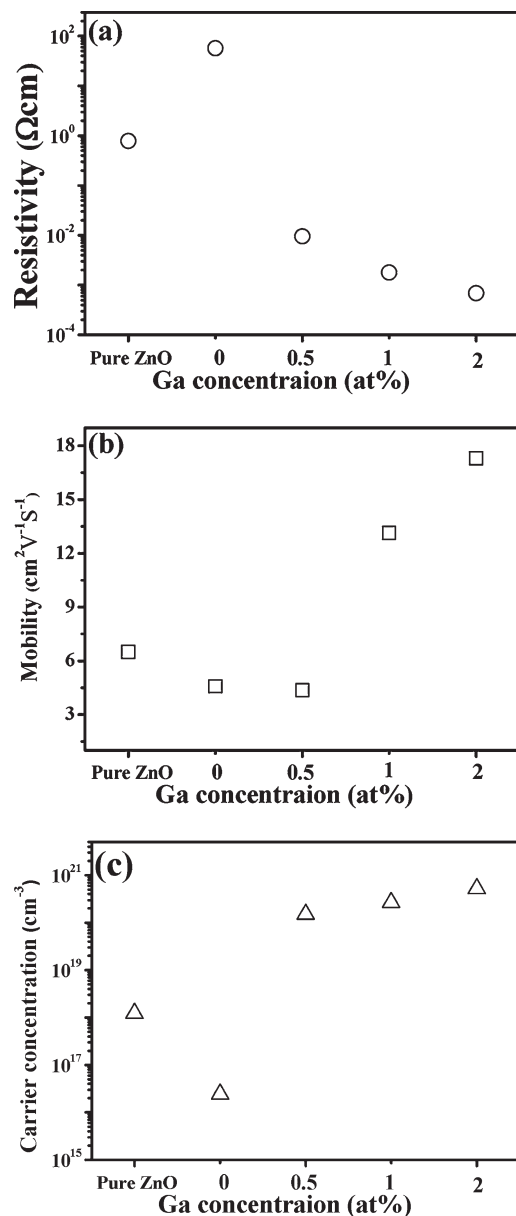
Figure 2 shows the XPS spectra of $\text{M}_x\text{G}_y\text{Z}_z\text{O}$ ($x = 0.05$, $y = 0.005$, and $z = 0.945$) thin films and two inserted figures show the Mg 2p and Ga 2p core levels. A typical survey spectrum of MGZO thin films confirmed the presence of Mg, Ga, Zn, and O

from MGZO films, as well as C from the reference. The binding energy of the Mg 2p core level of MGZO thin film was observed at 50.6 eV.¹⁷ The observed binding energy peaks located at 1117.9 and 1144.9 eV of MGZO thin film coincided with the electronic state of Ga 2p_{3/2} and 2p_{1/2} core levels, respectively.¹⁶ The different Ga concentration in the XPS spectra was similar at a Ga concentration of 1 at% and 2 at%. XPS studies showed that Ga–O and Mg–O bonds are evident but there was no significance of Ga and Mg metallic bonds indicating that the Ga^{3+} and Mg^{2+} ions located at Zn^{2+} sites in the MGZO crystal structure.

Figure 3 shows the titled view FE-SEM images of pure ZnO (a), MZO (b), and MGZO (c–e) thin films with different Ga concentrations. It was observed that the interfaces between the pure ZnO, MZO, and MGZO thin films, and the glass substrates

Table 1. Compositional Ratio of Pure ZnO, MZO, and MGZO Thin Films Deposited with Different Ga Concentrations

	Zn (at %)	O (at %)	Mg (at %)	Ga (at %)	total (%)
pure ZnO	49.78	50.22			100
Mg _{0.05} Zn _{0.95} O	43.30	51.96	4.74		100
Mg _{0.05} Ga _{0.005} Zn _{0.945} O	44.88	49.72	4.91	0.49	100
Mg _{0.05} Ga _{0.01} Zn _{0.94} O	42.78	49.08	4.98	1.16	100
Mg _{0.05} Ga _{0.02} Zn _{0.93} O	43.97	49.01	4.92	2.1	100

**Figure 4.** Variation of the resistivity (a), mobility (b), and carrier concentration (c) of the pure ZnO, MZO, and MGZO thin films deposited at different Ga concentration.

were very sharp without any indication of an interfacial reaction and the formation of interfacial compounds. The pure ZnO,

MZO, and MGZO thin films had a dense, uniform, and crack-free microstructure. The individual grains with a columnar shape were clearly observed regardless of the Ga concentration. The morphology of MGZO thin films had smoother surface, and this nature improved with increasing Ga concentration. Furthermore, these films were smoother surface than pure ZnO and MZO thin films. The grain size of the MGZO thin films decreased with increasing Ga concentration, which was smaller than that of pure ZnO and MZO films. Similar results have been reported in our previous papers.^{14,18,19} This behavior was attributed to the various relationships between the nucleation, growth and activation energy of the thin films.¹⁷ When the elements were doped in the ZnO crystal structure, the activation energy for nucleation and growth in the MZO or MGZO thin film was higher than that of pure ZnO.

Table 1 shows the compositional analysis of pure ZnO, MZO, and MGZO thin films. It was observed that the compositional ratio of pure ZnO, MZO, and MGZO thin films were slightly deviated from those of the ceramic targets. The Ga atomic ratio of MGZO thin films increased from 0.49 to 2.1 at % with increasing Ga concentration. The oxygen (O) atomic ratio of pure ZnO and MGZO thin films was below 50% except to that of MZO.

Figure 4 shows the variation of electrical resistivity (a), mobility (b), and carrier concentration (c) of the pure ZnO, MZO, and MGZO thin films deposited at different Ga concentrations. The values of electrical resistivity, mobility, and carrier concentration of pure ZnO thin films were $7.8 \times 10^{-1} \Omega\text{cm}$, $6.49 \text{ cm}^2\text{V}^{-1}\text{s}^{-1}$, and $1.23 \times 10^{18} \text{ cm}^{-3}$, whereas these values for MZO were $5.7 \times 10^1 \Omega\text{cm}$, $4.57 \text{ cm}^2\text{V}^{-1}\text{s}^{-1}$, and $2.45 \times 10^{16} \text{ cm}^{-3}$, respectively. The poor electrical characteristics of the MZO thin films were attributed to the low carrier concentration. The compositional study showed a relative higher O atomic ratio in the MZO thin films (Table 1), which leads to a low carrier concentration from O vacancies in MZO films. This electrical behavior was attributed to the same ionic charge of both Zn^{2+} and Mg^{2+} , indicating that the Mg^{2+} ions in the MZO thin films can't be generated by excess carrier concentrations.¹⁰ In addition, it is observed that the electrical mobility of $\text{M}_{0.05}\text{G}_{0.005}\text{Z}_{0.945}\text{O}$ has lower mobility than that of MZO. This characteristic is attributed to the higher carrier concentrations of $\text{M}_{0.05}\text{G}_{0.005}\text{Z}_{0.945}\text{O}$ than that of MZO. This higher carrier concentration in the thin film acts as free electron scattering centers, leading to a decrease in the electrical mobility.¹⁴ Therefore, the $\text{M}_{0.05}\text{G}_{0.005}\text{Z}_{0.945}\text{O}$ thin film with high concentration has lower mobility than that of MZO.

However, the electrical resistivity, mobility and carrier concentration of the MGZO thin films improved from 9.5×10^{-2} to $6.89 \times 10^{-4} \Omega\text{cm}$, 4.35 to $17.3 \text{ cm}^2\text{V}^{-1}\text{s}^{-1}$, and 1.5×10^{20} to $5.23 \times 10^{20} \text{ cm}^{-3}$, respectively, with increasing Ga concentration from 0.5 to 2 at %. This improved carrier concentration of the MGZO thin films can be attributed to the partial substitution of Zn^{2+} ions by Ga^{3+} ions, where each substituted atom generates one free electron in the conduction band, which results in an increase in carrier concentration.¹⁵ At band energy structure, the filled bottom of the conduction band at high carrier concentration resulted in the higher ionization energy indicating the increase in the value band gap energy.⁴ In particular, the $\text{M}_{0.05}\text{G}_{0.02}\text{Z}_{0.93}\text{O}$ thin film with highest carrier concentrations released a metallic behavior, which formats a degenerate band appearing in heavily doped semiconductors.²⁰ On the other hands, the outstanding mobility of $\text{M}_{0.05}\text{G}_{0.02}\text{Z}_{0.93}\text{O}$ thin film compared to that of MGZO using 0.5 at% Ga concentration resulted from the improvement in crystallinity. Our previous

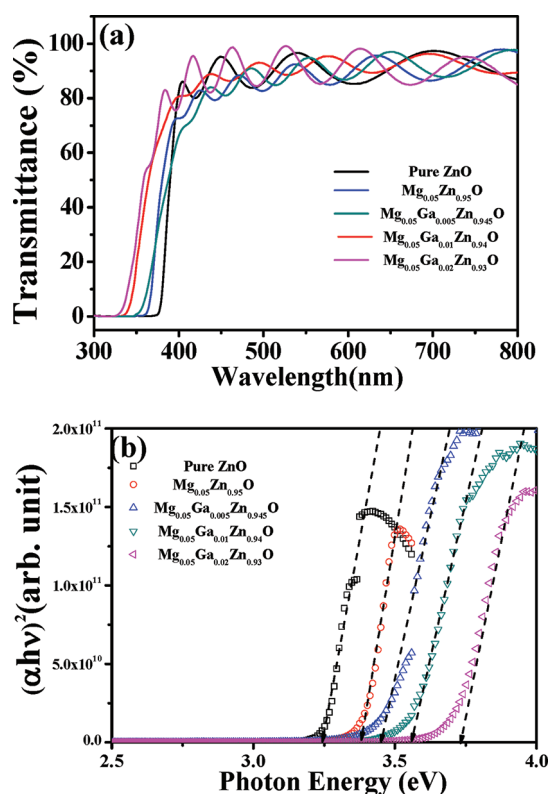


Figure 5. UV–visible transmittance spectra (a) in the wavelength region from 300 to 800 nm and the plot of $(\alpha h\nu)^2$ vs photon energy ($h\nu$) (b) of the pure ZnO, MZO and MGZO thin films deposited at different Ga concentration.

work showed the nature of defects and grain boundaries of different thin films were strongly dependent on the crystal quality.^{13,18} The crystal quality of the film was poor with many defects and grain boundaries.¹⁴ The defects and grain boundary acted as free electron trap centers, which reduced the charge carrier concentration and became scattering centers for electron transport, leading to a decrease in electrical mobility.¹⁹ The surface morphology of the thin film is related to the electrical mobility of the thin film. The rough surface morphology also reduces the mean free path of free electrons on surface of the thin film, leading to an increase in surface resistivity.²⁰ Therefore, MGZO thin films containing 2 at % Ga showed improved electrical properties compared to that containing 0.5 at % Ga.

Figure 5 shows the UV–visible transmittance spectra (a) from 300 to 800 nm along with a plot of $(\alpha h\nu)^2$ vs photon energy ($h\nu$) (b) of the pure ZnO, MZO, and MGZO thin films synthesized with different Ga concentrations. The pure ZnO, MZO, and MGZO thin films showed high transmittance (varying from 70% to 95%) in the visible region (Figure 5a). The absorption edge of all the deposited thin films was quite sharp and was found to depend on the Ga concentration. The absorption edge of the MGZO thin film shifted toward a lower wavelength side from 375 to 324 nm with increasing Ga concentration. The shift in the absorption edge was responsible for the improved optical transmittance in the lower wavelength region as compared to that of the pure ZnO thin films. The optical band gap energy (E_g) of pure ZnO, MZO, and MGZO thin films was measured by a linear extrapolation on x -axis of the $(\alpha h\nu)^2$ versus photon energy ($h\nu$) plot. The band gap of the films was found to be dependent

on the Ga concentration (Figure 5b). When the Ga concentration was increased, the E_g of the MGZO thin films increased from 3.45 to 3.75 eV as compared to that of ZnO (3.25 eV) and MZO (3.4 eV). These E_g values of the MGZO thin films were wider than that of reported for pure ZnO, $\text{Mg}_{0.05}\text{Zn}_{0.95}\text{O}$, and $\text{Ga}_{0.02}\text{Zn}_{0.98}\text{O}$ thin films, respectively^{8,18} and can be explained by the Burstein–Moss effect.²¹ This behavior was in good agreement to the improved carrier concentration (Figure 4 (c)). From the aforementioned discussion, it is concluded that MGZO thin films with outstanding optical and electrical characteristics compared to the pure ZnO, MZO and Group III element-doped ZnO can be easily applied in different optoelectronic devices, such as TFSCs and ultraviolet LEDs because of improved performance in the form of higher transmittance in the short wavelength, wider band gap energy, and improved electrical properties.

4. CONCLUSION

Quaternary Mg and Ga codoped ZnO (MGZO) thin films with transparent conducting characteristics on glass substrates can be designed systematically, grown by RF sputtering and characterized in detail. The properties of the MGZO thin films are strongly dependent on the Ga concentration. The lowest electrical resistivity of $6.89 \times 10^{-4} \Omega \text{ cm}$ and the wider band gap energy of 3.75 eV can be obtained for MGZO thin film deposited at 2 at % Ga concentration. These interesting properties of MGZO thin films enumerates the vital characteristics of a promising candidate that can be used as window layer in TFSCs and n-type layer in ultraviolet LEDs.

AUTHOR INFORMATION

Corresponding Author

*E-mail: jinhyeok@chonnam.ac.kr (J.H.K.); j.y.lee@kaist.ac.kr (J.Y.L.). Phone: 82-62-530-1709 (J.H.K.); 82-42-350-4216 (J.Y.L.). Fax: 82-62-530-1699 (J.H.K.); 82-42-350-3310 (J.Y.L.).

ACKNOWLEDGMENT

This study was funded partially by the Korea Institute of Industrial Technology (KITECH), National Research Foundation of Korea (NRF) grant funded by the Korean government (MEST-No. 2011-0001002) and Ho-Nam Leading industry office through the Leading Development for Economic Region.

REFERENCES

- (1) Kato, H.; Sano, M.; Miyamoto, K.; Yao, T. *J. Cryst. Growth* **2002**, 237–239 (Part 1), 538–543.
- (2) Ahn, B. D.; Oh, S. H.; Lee, C. H.; Kim, G. H.; Kim, H. J.; Lee, S. Y. *J. Cryst. Growth* **2007**, 309, 128–133.
- (3) Kim, S.; Lee, W. I.; Lee, E. H.; Hwang, S. K.; Lee, C. *J. Mater. Sci.* **2007**, 42, 4845–4849.
- (4) Michael, S.; Tiwari, A. *J. Appl. Phys.* **2007**, 101, 124912–124918.
- (5) Yang, W.; Vispute, R. D.; Choopun, S.; Sharma, R. P.; Venkatesan, T.; Shen, H. *Appl. Phys. Lett.* **2001**, 78, 2787–2789.
- (6) Choopun, S.; Vispute, R. D.; Yang, W.; Sharma, R. P.; Venkatesan, T.; Shen, H. *Appl. Phys. Lett.* **2002**, 80, 1529–1531.
- (7) Kaushal, A.; Kaur, D. *Sol. Energy Mater. Sol. Cells* **2009**, 93 (2), 193–198.
- (8) Shimakawa, S.; Hashimoto, Y.; Hayashi, S.; Satoh, T.; Negami, T. *Sol. Energy Mater. Sol. Cells* **2008**, 92, 1086–1090.
- (9) Schmidt-Grund, R.; Carstens, A.; Rheinlander, B.; Spemann, D.; Hochmut, H.; Zimmermann, G.; Lorenz, M.; Grundmann, M.; Herzinger, C. M.; Schubert, M. *J. Appl. Phys.* **2006**, 99, 123701–123707.

- (10) Minemoto, T.; Hashimoto, Y.; Satoh, T.; Negami, T.; Takakura, H.; Hamakawa, Y. *J. Appl. Phys.* **2001**, *89*, 8327–8330.
- (11) Chen, X. L.; Xu, B. H.; Xue, J. M.; Zhao, Y.; Wei, C. C.; Sun, J.; Wang, Y.; Zhang, X. D.; Geng, X. H. *Thin Solid Films* **2007**, *515*, 3753–3759.
- (12) Guillen, C.; Herrero, J. *Thin Solid Films* **2006**, *515*, 640–643.
- (13) Shin, S. W.; Lee, G. H.; Moholkar, A. V.; Moon, J. H.; Heo, G. S.; Kim, T. W.; Kim, J. H.; Lee, J. Y. *J. Cryst. Growth* **2011**, *322*, 51–56.
- (14) Shin, S. W.; Sim, K. U.; Pawar, S. M.; Moholkar, A. V.; Jung, I. O.; Yun, J. H.; Moon, J. H.; Kim, J. H.; Lee, J. Y. *J. Cryst. Growth* **2010**, *312*, 1551–1556.
- (15) Kim, K. H.; Park, K. C.; Ma, D. Y. *J. Appl. Phys.* **1997**, *81*, 7764–7772.
- (16) Wei, W.; Jin, C.; Narayan, J.; Narayan, R. *J. Solid State Commun.* **2009**, *149*, 1670–1673.
- (17) Huang, H. H.; Chu, S. Y.; Kao, P. C.; Chen, Y. C. *Thin Solid Films* **2008**, *516*, 5664–5668.
- (18) Sim, K. U.; Shin, S. W.; Moholkar, A. V.; Yun, J. H.; Moon, J. H.; Kim, J. H. *Curr. Appl. Phys.* **2010**, *10*, S463–S467.
- (19) Kim, D. H.; Jeon, H. H.; Kim, G. C.; Hwangboe, S. J.; Verma, V. P.; Choi, W. B.; Jeon, M. H. *Opt. Commun.* **2008**, *281*, 2120–2125.
- (20) Bhosle, V.; Tiwari, A.; Narayan, J. *J. Appl. Phys.* **2006**, *100*, 033713–033716.
- (21) Chen, Z.; Fang, G.; Li, C.; Sheng, S.; Jie, G.; Zhao, X. Z. *Appl. Surf. Sci.* **2006**, *252*, 8657–8661.